

The 1-MeV electron irradiation effect and damage mechanism analysis of GaInP/GaAs heterojunction solar cells

Kelun Zhao(赵克伦), Jiaming Zhou(周佳明), Yanqing Zhang(张延清), Qiang Kang(康强), Yang Liu(刘洋), Xinyi Li(李欣益), Chaoming Liu(刘超铭), Tianqi Wang(王天琦), and Mingxue Huo(霍明学)

Citation: Chin. Phys. B, 2026, 35 (**4**): 048801. DOI: 10.1088/1674-1056/ae0638
http://cpb.iphy.ac.cn; http://iopscience.iop.org/cpb

What follows is a list of articles you may be interested in

Band engineering and recombination mechanisms in lead-free perovskite solar cells

Wei Liu(刘维), Tingxue Zhou(周庭雪), Liang Chu(楚亮), and Xing'ao Li(李兴鳌)
Chin. Phys. B, 2026, 35 (**2**): 028801. DOI: 10.1088/1674-1056/ae156b

SolarDesign: An online photovoltaic device simulation and design platform

Wei E. I. Sha(沙威), Xiaoyu Wang(王啸宇), Wenchao Chen(陈文超), Yuhao Fu(付钰豪), Lijun Zhang(张立军), Liang Tian(田亮), Minshen Lin(林敏慎), Shudi Jiao(焦书迪), Ting Xu(徐婷), Tiange Sun(孙天歌), and Dongxue Liu(刘冬雪)
Chin. Phys. B, 2025, 34 (**1**): 018801. DOI: 10.1088/1674-1056/ad9017

Degradation behavior of electrical properties of GaInAs (1.0 eV) and GaInAs (0.7 eV) sub-cells of IMM4J solar cells under 1-MeV electron irradiation

Yan-Qing Zhang(张延清), Ming-Xue Huo(霍明学), Yi-Yong Wu(吴宜勇), Cheng-Yue Sun(孙承月), Hui-Jie Zhao(赵慧杰), Hong-Bin Geng(耿洪滨), Shuai Wang(王帅), Ru-Bin Liu(刘如彬), Qiang Sun(孙强)
Chin. Phys. B, 2017, 26 (**8**): 088801. DOI: 10.1088/1674-1056/26/8/088801

β-$FeSi_2$ as the bottom absorber of triple-junction thin-film solar cells：A numerical study

Yuan Ji-Ren (袁吉仁), Shen Hong-Lie (沈鸿烈), Zhou Lang (周浪), Huang Hai-Bin (黄海宾), Zhou Nai-Gen (周耐根), Deng Xin-Hua (邓新华), Yu Qi-Ming (余启名)
Chin. Phys. B, 2014, 23 (**3**): 038801. DOI: 10.1088/1674-1056/23/3/038801

odified-DBR-based semi-omnidirectional multilayer anti-reflection coating for tandem solar cells

Ali Bahrami, Shahram Mohammadnejad, Nima Jouyandeh Abkenar
Chin. Phys. B, 2014, 23 (**2**): 028803. DOI: 10.1088/1674-1056/23/2/028803

The 1-MeV electron irradiation effect and damage mechanism analysis of GaInP/GaAs heterojunction solar cells

Kelun Zhao(赵克伦)[1], Jiaming Zhou(周佳明)[2], Yanqing Zhang(张延清)[3,†], Qiang Kang(康强)[1], Yang Liu(刘洋)[4], Xinyi Li(李欣益)[4], Chaoming Liu(刘超铭)[2], Tianqi Wang(王天琦)[3], and Mingxue Huo(霍明学)[2,‡]

[1] *School of Physics, Harbin Institute of Technology, Harbin* 150001, *China*
[2] *School of Astronautics, Harbin Institute of Technology, Harbin* 150001, *China*
[3] *Space Environment Simulation Research Infrastructure, Harbin Institute of Technology, Harbin* 150001, *China*
[4] *Shanghai Institute of Space Power Sources, Shanghai* 200245, *China*

(Received 10 July 2025; revised manuscript received 18 August 2025; accepted manuscript online 12 September 2025)

This study explore the radiation damage effects on GaInP/GaAs heterojunction (HJT) solar cells when subjected to 1-MeV electron irradiation. Light *I*–*V* measurements show that V_{oc}, J_{sc}, and P_{max} of the cells exhibit a logarithmic degradation pattern with increasing electron irradiation fluence. Under identical irradiation conditions, the degradation of J_{sc} is substantially less pronounced than that of V_{oc}. Under the same conditions, the heterojunction cell shows better radiation resistance, mainly as its V_{oc} degradation rate with fluence increase is lower than the homojunction cell. Spectral response analysis reveals that 1-MeV electron radiation mainly causes longwave zone damage in the GaInP/GaAs HJT cells, which intensifies as irradiation fluence accumulates. Dark characteristic analysis indicates that both recombination and diffusion currents in the cells rise with increasing irradiation fluence, with recombination current dominating the dark current. Deep level transient spectroscopy tests show that 1-MeV electron irradiation introduces four defects (H_1–H_4) in the cells, located at H_1 ($E_v+0.717$ eV)/H_1^* ($E_v+0.744$ eV), H_2 ($E_v+0.369$ eV), H_3 ($E_v+0.282$ eV), and H_4 ($E_v+0.032$ eV). Among these, the concentration H_1 of defects increases most drastically with fluence and directly correlates with the rapid degradation of cell performance under high fluence, making it the crucial factor responsible for the swift degradation of GaInP/GaAs HJT cells under high fluence 1-MeV electron irradiation.

Keywords: 1-MeV electron radiation, GaInP/GaAs HJT solar cell, deep level transient spectroscopy (DLTS)

PACS: 88.40.jp, 88.40.H–, 88.40.fh

DOI: 10.1088/1674-1056/ae0638 **CSTR:** 32038.14.CPB.ae0638

1. Introduction

In the past half century, solar cells have become a main energy source for space exploration spacecraft since NASA first applied photovoltaic technology to satellites. As human exploration extends to deep space, space-specific solar cells face challenges from extreme environments like temperature cycles and radiation.[1–4] Recent progress in photovoltaic materials, such as wider temperature adaptability and better radiation resistance,[5–7] has driven high conversion efficiency photovoltaic arrays forward remarkably. Advanced photovoltaic systems, with great radiation resistance and long term stability, are key for space exploration power.[8–10] Among photovoltaic tech, III–V group solar cells, particularly GaAs ones, are crucial in multi-junction cells and widely used in spacecraft power systems due to their radiation resistance and adaptability.[11,12] Research shows that for GaInP/GaAs/Ge three-junction solar cells, radiation damage mainly affects the GaAs sub-cell, whose fast degradation limits the overall cell efficiency.[13–15] 1-MeV electron irradiation causes the EOL J_{sc} of the GaAs sub-cell in the GaInP/GaAs double-junction cell to drop to 83% of its initial value,[16,17] in the GaInP/GaAs/Ge triple-junction cell, the EOL J_{sc} retention rate of its GaAs sub-cell reaches 93%.[18,19] As space exploration missions grow more demanding, solar cells need better performance, especially stability in high energy particle radiation. Recently, heterojunction solar cell technology has gained attention for optimizing GaAs solar cell design to meet these complex space mission needs.

GaInP/GaAs HJT solar cells, a promising photovoltaic tech, leverage high/low bandgap semiconductor interfaces for a simple hetero p–n junction. Their excellent passivation contact and stability make them a likely next-gen mainstream product.[20,21] They outperform homojunction cells in efficiency due to dark current's exponential drop with p–n junction bandgap rise, driven by non-equilibrium carrier recombination and non-radiative SRH recombination. This phenomenon impacts the open-circuit voltage more than the short-circuit current, thereby enhancing the cell's efficiency.[22] KL Schulte's team modeled and simulated GaAs heterojunction

†Corresponding author. E-mail: yqzhang1983@hit.edu.cn
‡Corresponding author. E-mail: huomingxue@hit.edu.cn

© 2026 Chinese Physical Society and IOP Publishing Ltd. All rights, including for text and data mining, AI training, and similar technologies, are reserved.

solar cells, finding that emitter doping and band offset are key for efficiency. They designed a GaAs/GaInPAs cell via HVPE with 27% efficiency under AM1.5 (1 Sun).[22] Antonio Marti's modeling showed heterojunction cells' open-circuit voltage can exceed the low-bandgap semiconductor's bandgap under finite carrier mobility.[23] Hwang *et al.* built an AlGaAs/GaAs cell with a logarithmic bandgap grading layer, achieving 28.7% efficiency via AFORS-HET optimization. This proved collaborative heterojunction and bandgap grading layer design boosts solar cell performance.[24] In space, abundant free charged particles are bound by planetary magnetic fields, forming radiation belts. Solar cells on orbiting spacecraft are exposed to radiation from these particles, causing a decline in their electrical performance.[25–31] Wang *et al.* used DLTS to study GaInP/GaAs/InGaAs IMM3J solar cells after 1-MeV electron irradiation. They found GaAs sub-cell defects at $E_v+0.36$ eV/$E_v+0.42$ eV and InGaAs sub-cell defects at $E_v+0.29$ eV/$E_v+0.24$ eV. DLTS results showed effective minority carrier lifetime in GaAs/InGaAs cells decreased with increasing irradiation fluence.[19] Zhou *et al.* used DLTS to study InGaAs (1.0 eV/0.7 eV) cells in IMM4J solar cells after 5-MeV proton irradiation. They found radiation introduced H ($E_v+0.09$ eV) and H_1 ($E_v+0.07$ eV) hole traps, with defect concentrations increasing with higher fluences.[31] These research findings underscore the significance of gaining a deep understanding of radiation damage mechanisms for optimizing solar cell structures and enhancing their radiation resistance.

To conduct an in-depth analysis of the radiation resistance performance of GaInP/GaAs heterojunction solar cells. In this work, this paper conducts 1-MeV electron radiation experiments on cells at varying fluences, simulating space radiation conditions. Using optical IV (LIV), external quantum efficiency (EQE), dark characteristics (DIV), and deep-level transient spectroscopy (DLTS) techniques, the study analyzes the cells' electrical, spectral degradation, and defect evolution before and after radiation.

2. Experiment

GaInP/GaAs heterojunction (HJT) solar cell with a size of 0.6 cm×0.6 cm was epitaxially grown on GaAs substrate using the metal organic chemical vapor deposition (MOCVD) technique. The structural schematic is shown in Fig. 1. The emitter region comprises high bandgap GaInP, while the base region consists of low bandgap GaAs. To mitigate the adverse effects of band discontinuity at the heterojunction interface on carrier drift, the emitter was heavily doped during growth to enhance the depletion region electric field. Additionally, a window layer and a back surface field (BSF) layer were incorporated to improve spectral utilization and carrier collection efficiency. Figure 2 shows the *I–V* characteristic curve of the GaInP/GaAs HJT solar cell before radiation under the standard test environment (AM0, 135.3 mW/cm^2, 25 ± 2 °C). This curve directly reflects the initial photovoltaic performance parameters of the GaInP/GaAs HJT solar cell, including a short-circuit current (I_{sc}) of 11.07 mA, an open-circuit voltage (V_{oc}) of 1.01 V, and a maximum power (P_{max}) of 8.65 mW. Based on these parameters, the power conversion efficiency of the GaInP/GaAs HJT solar cell is 17.8%, fully demonstrating its excellent energy conversion performance.

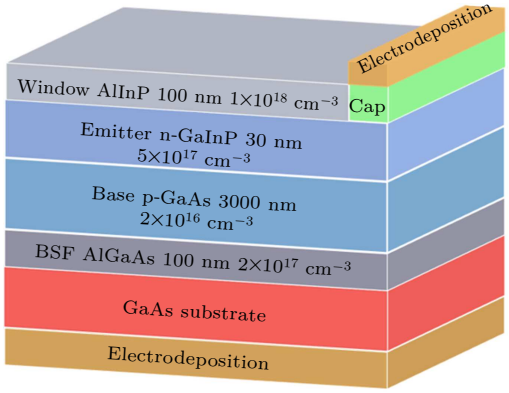


Fig. 1. Schematic diagram of the GaInP/GaAs heterojunction solar cell structure.

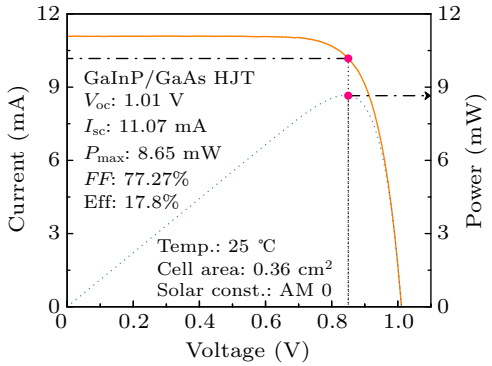


Fig. 2. Before radiation, the light *I–V* curve of the GaInP/GaAs heterojunction solar cell under standard conditions.

This study conducted irradiation experiments on GaInP/GaAs HJT solar cells using 1-MeV electron accelerator at the Heilongjiang Institute of Nuclear Energy. At room temperature, irradiation experiments were carried out on GaInP/GaAs HJT cells with radiation fluxes of 1×10^{11} cm^{-2}·s^{-1} and fluences of 1×10^{14} cm^{-2}, 3×10^{14} cm^{-2}, 5×10^{14} cm^{-2}, 8×10^{14} cm^{-2}, and 1×10^{15} cm^{-2} at 1-MeV electrons. Following irradiation, samples underwent 3-day RT annealing. Post-annealing electrical performance was measured under standard test conditions (AM0, 135.3 mW/cm^2, 25 ± 2 °C). Spectral response (external quantum efficiency, EQE) was measured as a function of irradiation fluence, and the scanning step size of the QE test is 5 nm. Dark current–voltage (DIV) characteristics, measured via the four-probe method to minimize series resistance

effects, were fitted with a double-exponential diode model to extract recombination parameters. Deep level transient spectroscopy (DLTS) was employed to analyze defect evolution post-irradiation. In the DLTS test, the reverse bias voltage U_R was set to 5 V, the pulse voltage U_p was set to 0.1 V, the pulse width t_p was set to 0.2 ms, and t_w was set to 19.2 ms, 192 ms, and 1.92 s.

3. Results and discussion

3.1. Analysis of light *I*–*V* characteristics

Figure 3(a) presents the light *I*–*V* characteristic curve of the GaInP/GaAs HJT solar cell after 1-MeV electron irradiation. From the figure, it can be seen that at room temperature, the 1-MeV electron irradiation causes a certain degree of damage to the electrical performance of the cell, and the degree of damage is positively correlated with the irradiation fluence. As the irradiation fluence increases, the degradation of the cell's electrical performance becomes more significant. This is because the number of displacement defects generated during the 1-MeV electron radiation increases rapidly with the increase in the irradiation fluence, thereby accelerating the recombination rate of photogenerated electron–hole pairs and leading to a significant decline in the cell's electrical performance. To present the damage effect of electron irradiation on the solar cell more intuitively, this paper normalizes the key parameters of the solar cell (J_{sc}, V_{oc}, P_{max}). A large number of studies have shown that the degradation of the solar cell's electrical performance has a logarithmic relationship with the irradiation fluence.[24,25] The degradation follows the empirical model

$$P = 1 - c_p \log\left(1 + \frac{\varphi}{\varphi_{0p}}\right), \tag{1}$$

where P represents the normalized electrical performance parameter; c_p is the performance degradation rate, which is usually limited to a dimensionless constant within the range of 0–1 during the fitting process; φ_{0p} is the critical fluence, which is related to the intrinsic properties of the solar cell and the type of irradiation particle energy.

Figure 3(b) presents the normalized degradation curves of the three main electrical parameters for the GaInP/GaAs HJT solar cell post 1-MeV electron irradiation, with fitting parameters in Table 1.

Table 1. Fitting parameters of the degradation curves of the electrical performance parameters of GaInP/GaAs HJT solar cells after 1-MeV electron irradiation.

	J_{sc}	V_{oc}	P_{max}
c_p	0.24	0.05	0.26
φ_0	3.83×10^{14}	6.19×10^{12}	1.84×10^{14}

Equation (1) can fit the cell's electrical damage and output pattern well, with a coefficient of determination (R^2) above 0.99. The results show a positive correlation between the degradation of these parameters and the radiation fluence. At the same fluence, V_{oc} degrades more than J_{sc}. As shown in Table 1, the critical fluence of J_{sc} is 62 times that of V_{oc}. So, rapid V_{oc} attenuation is a key factor in the cell's performance degradation. When the cumulative irradiation fluence reaches 1×10^{15} cm^{-2}, further analysis shows that the J_{sc}, V_{oc}, and P_{max} of the GaInP/GaAs HJT solar cell degrade to 86.9%, 88.1%, and 78.6% of the initial values respectively. Notably, P_{max} degrades fastest as radiation fluence increases, since it's jointly impacted by V_{oc} and J_{sc} degradation. Despite this, the GaInP/GaAs HJT solar cell's power conversion efficiency remains at 13.8%, indicating its excellent radiation resistant performance.

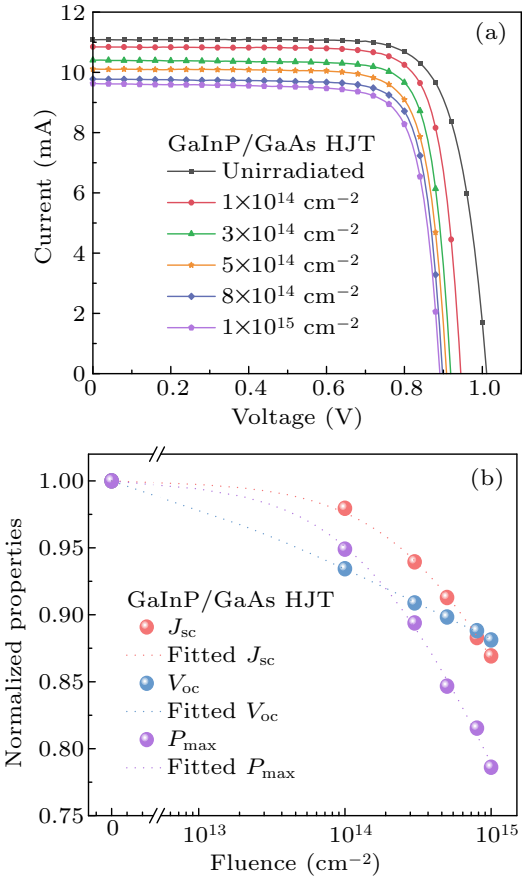


Fig. 3. After different fluences of 1-MeV electron radiation, for the GaInP/GaAs HJT solar cell (a) the LIV characteristic curve and (b) the degradation curves of the normalized electrical performance parameters with respect to the irradiation fluence.

Figure 4 compares the open-circuit voltage degradation trends of GaAs heterojunction and homojunction solar cells after 1-MeV electron irradiation. Under the same conditions, the heterojunction cell shows better radiation resistance, mainly as its V_{oc} degradation rate with fluence increase is lower than the homojunction cell. The heterostructure shifts part of the p–n junction depletion region to high-bandgap GaInP, lowering the

SRH recombination rate.[18] This inhibition reduces the V_{oc} degradation trend with radiation fluence increase, enhancing the cell's radiation resistance.

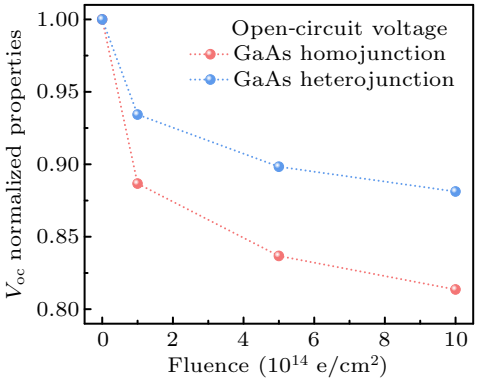


Fig. 4. Comparison chart of the normalized V_{oc} of GaInP/GaAs heterojunction and homojunction solar cells after irradiation with different fluences of 1-MeV electron radiation.

3.2. Analysis of external quantum efficiency

Figure 5(a) presents the spectral response curves of GaInP/GaAs HJT solar cells after irradiation with different fluences of 1-MeV electrons. As the fluence increases, the EQE decreases overall. Analysis of the spectral response degradation reveals that the radiation damage primarily manifests as reduced response in the long-wavelength band, with the degradation magnitude increasing with fluence. The 1-MeV irradiation energy is sufficient to generate displacement damage in GaInP/GaAs HJT solar cells. Given that the penetration depth of 1-MeV electrons exceeds the cell thickness, the damage distribution in the active region is uniform.[13,27] Based on the structure, where the GaAs base region is ~ 100 times thicker than the GaInP emitter, the damage is concentrated primarily in the GaAs base. As GaAs is a direct-bandgap semiconductor, photons penetrate deeper at longer wavelengths. Thus, photogenerated carriers produced by long-wavelength photons originate farther from the junction. This increases the probability of carrier capture by defects, explaining the long-wavelength band degradation observed.

Photocurrent density (J_{ph}), a key parameter for evaluating solar cell performance and material properties, is obtained from spectral response measurements. Figure 5(b) shows the normalized J_{ph} as a function of 1-MeV electron irradiation fluence. After irradiation, the degradation of J_{ph} is well described by Eq. (1), with the R^2 above 0.99. The fitting results reveal that the electrical performance degradation rate c_p of the J_{ph} fitting curve is 0.23, and the critical fluence is 3.63×10^{14} cm^{-2}. As shown in Fig. 5(b), as the irradiation fluence increases, J_{ph} degrades slowly initially; however, once the fluence exceeds 3.63×10^{14} cm^{-2}, the degradation rate increases significantly. When the irradiation fluence reaches 1×10^{15} cm^{-2}, J_{ph} still retains 87% of the initial performance of the GaInP/GaAs HJT solar cell. This further demonstrates that GaInP/GaAs HJT solar cells possess excellent radiation resistance performance.

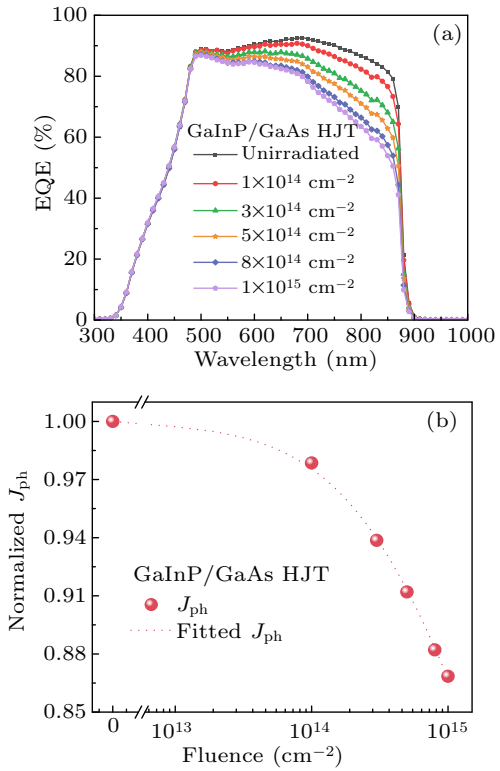


Fig. 5. After different fluences of 1-MeV electron radiation for GaInP/GaAs HJT solar cells: (a) spectral response curves and (b) the degradation curves of normalized J_{ph} with respect to irradiation fluence.

3.3. Analysis of dark *I–V* characteristic

To eliminate the interference of photogenerated carriers and deeply reveal the damage mechanism of GaInP/GaAs HJT solar cells under 1-MeV electron irradiation, and to quantitatively analyze the performance degradation law before and after irradiation, this study uses a double-exponential model to fit and analyze the dark characteristic curve. This model splits the reverse saturation current into two components: diffusion current (J_{diff}) and recombination current (J_{rec}), thereby more effectively characterizing the intrinsic performance of the solar cell. The equation is expressed as

$$J_L = J_{diff}\left(\exp\frac{U-J_LR_s}{A_1U_T}-1\right) + J_{rec}\left(\exp\frac{U-J_LR_s}{A_2U_T}-1\right)-\frac{U-J_LR_s}{R_{sh}}. \quad (2)$$

Among them $A_1 = n_1/KT$, $A_2 = n_2/KT$, n_1 and n_2 represent the diffusion ideality factor and the recombination ideality factor respectively. Series resistance (R_s) and shunt resistance (R_{sh}) represent the series and parallel resistive losses, respectively. Measurements using the four-probe method minimized contact and series resistance effects, ensuring consistency across the batch of GaInP/GaAs HJT solar cells studied. Before and after irradiation measurements showed $R_s <$

0.1 Ω·cm^2 and $R_{sh} > 10^6$ Ω·cm^2. Therefore, in this experiment, R_s and R_{sh} were not the main influencing factors of the dark current of the solar cell, and they were ignored in the subsequent analysis. Figure 6 shows the DIV of GaInP/GaAs HJT solar cells under different irradiation fluences of 1-MeV electrons. From the figure, two typical features can be observed: (i) When the scanning voltage is lower than the forward turn on voltage, the current remains at a low level; (ii) After the voltage crosses the forward turn on threshold, the current increases linearly, indicating that the device enters the low resistance working region. It is worth noting that as the electron irradiation fluence increases, the dark characteristic curve shifts overall towards lower voltage and higher current. This indicates that with the increase of irradiation fluence, the dark current increases significantly under the same forward bias voltage.

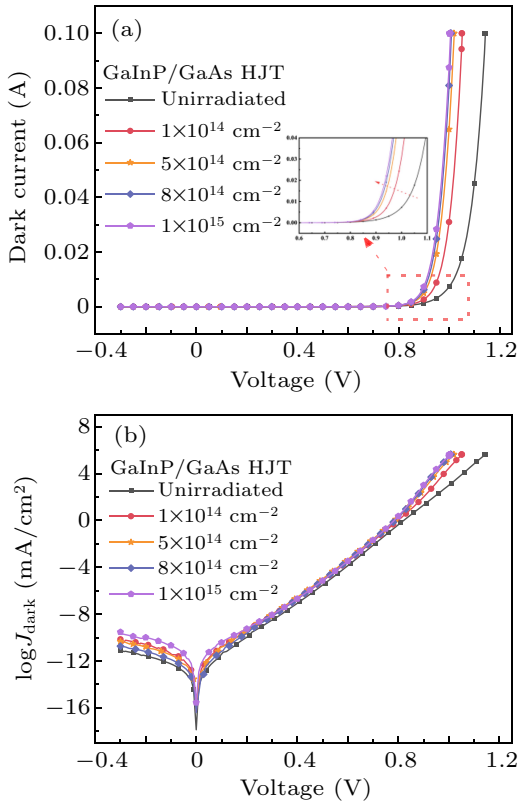


Fig. 6. DIV curve of GaInP/GaAs heterojunction solar cell after 1-MeV electron irradiation.

To simplify curve fitting and enhance accuracy, the diffusion ideality factor n_1 was set to 1. Table 2 lists the fitted parameters of the DIV curves under various irradiation fluences obtained from the double-exponential model. Figure 7 reveals the trends of diffusion current J_{diff} and recombination current J_{rec} with irradiation fluence. From Fig. 7(a), J_{diff} increases significantly with rising irradiation fluence. This stems from irradiation induced reduction in minority carrier diffusion length (L_p) which directly elevates J_{diff}. Since J_{diff} is governed by carrier recombination within a characteristic distance L_p from the space charge region edge,[32] defect accumulation near the junction enhances recombination, further increasing J_{diff}. Under 1-MeV electron irradiation, GaInP/GaAs HJT solar cells show uniform radiation damage defect distribution. With the introduction of irradiation defects, the effective number of minority carriers that can migrate to the junction region is reduced, resulting in a decrease in the short-circuit current. This mechanism is highly consistent with the J_{sc} change trend shown in Fig. 3, revealing that the abnormal increase in diffusion current is one of the key factors causing the degradation of the short-circuit current. Figure 7(b) experimentally shows a strong positive correlation between J_{rec} and 1-MeV electron irradiation fluence. This current component originates from Shockley–Read–Hall (SRH) nonradiative recombination via defects in the space charge region.[33] Under 1-MeV electron irradiation, the space charge region defect concentration rises with fluence, amplifying recombination center density. These centers reduce minority carrier lifetime (τ) through enhanced SRH recombination, thereby elevating J_{rec}. Further analysis reveals that when the radiation fluence reaches 1×10^{15} cm^{-2}, the J_{diff} and J_{rec} of the GaInP/GaAs heterojunction are approximately increased to 130 times and 1.6 times of the initial values, respectively. The maximum J_{diff} is of the order of 10^{-17}, and the maximum J_{rec} is of the order of 10^{-9}. J_{rec} is more than 10^8 times that of J_{diff}. Thus, after 1-MeV electron irradiation, the dark current of the GaInP/GaAs heterojunction solar cell is dominated by the recombination current.

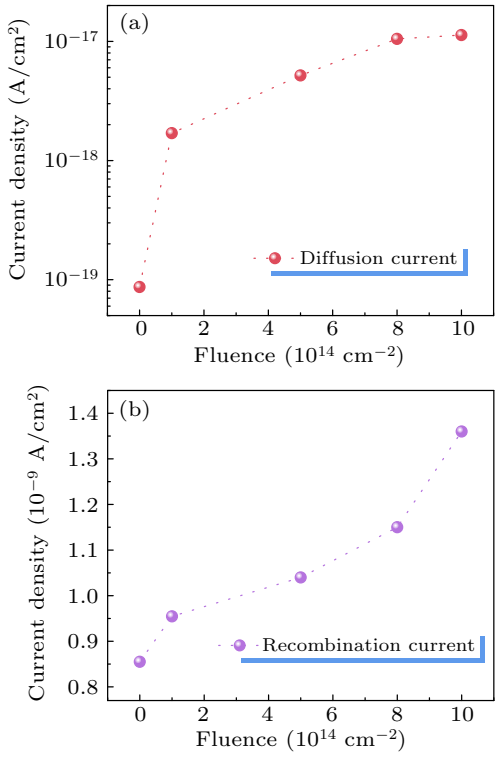


Fig. 7. The trend of diffusion current J_{diff} and recombination current J_{rec} of GaInP/GaAs heterojunction solar cells after 1-MeV electron irradiation with the variation of irradiation fluence.

Table 2. Fitting parameters of the DIV curve for GaInP/GaAs HJT solar cells after 1-MeV electron irradiation.

	J_{diff} (A/cm^2)	J_{rec} (A/cm^2)	n_1	n_2
Unirradiated	8.68×10^{-20}	8.55×10^{-10}	1	2.28
1×10^{14}	1.70×10^{-18}	9.55×10^{-10}	1	2.26
5×10^{14}	5.18×10^{-18}	1.04×10^{-9}	1	2.23
8×10^{14}	1.05×10^{-17}	1.15×10^{-9}	1	2.22
1×10^{15}	1.13×10^{-17}	1.36×10^{-9}	1	2.21

3.4. Deep-level transient spectroscopy analysis

In solar cells, SRH recombination is the main factor affecting the diffusion of excess carriers. Defects induced during fabrication and irradiation act as recombination centers, accelerating SRH recombination, thus reducing carrier lifetime and degrading cell performance. Therefore, accurately characterizing the energy levels, concentrations and capture cross-sections of these defects is of great significance for deeply understanding the performance degradation of radiation-induced solar cells. The DLTS technique based on the capture and emission processes of carriers by deep-level traps, and through systematic temperature scanning and rate window analysis, can quantitatively measure and analyze key parameters such as the energy level positions, concentrations, and capture cross-sections of the defects.[34,35] So, in this study, we conducted systematic DLTS tests on GaInP/GaAs HJT solar cells under different irradiation fluences.

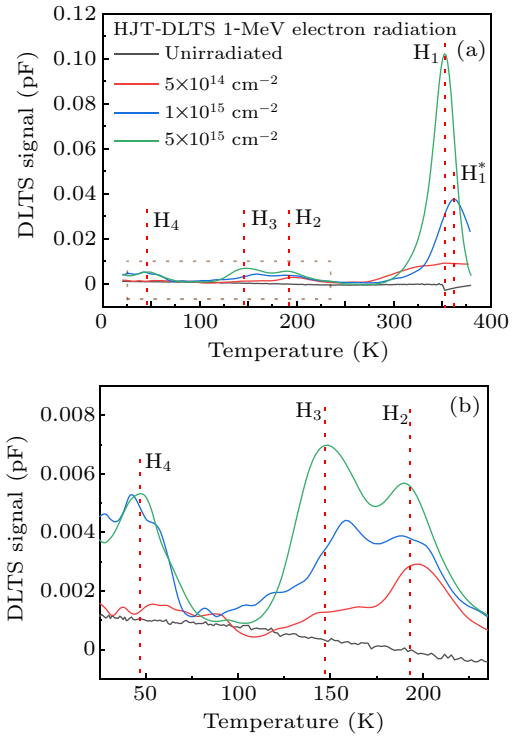


Fig. 8. DLTS curve of GaInP/GaAs heterojunction solar cell after 1-MeV electron irradiation: (a) DLTS test results, (b) magnified view.

Figure 8 shows the evolution of the DLTS spectra for the GaInP/GaAs HJT solar cell measured between 20 K–380 K as a function of irradiation fluence. The defect characteristics change significantly with fluence, manifested primarily by differing growth rates in the intensities of the characteristic defect peaks. Given that the sample structure used in this study is n^+p, the majority carriers in the low-doped base region are holes, so the four characteristic defect peaks shown in the figure all correspond to hole defects, and their energy levels are located above the valence band top. The DLTS analysis results show that 1-MeV electron irradiation conditions mainly introduce four characteristic hole defect peaks (H_1–H_4) in the GaInP/GaAs HJT solar cell. Their energy level positions are presented in Table 3: H_1 ($E_v+0.717$ eV)/H_1^* ($E_v+0.744$ eV), H_2 ($E_v+0.369$ eV), H_3 ($E_v+0.282$ eV), and H_4 ($E_v+0.032$ eV). Further analysis revealed that the concentrations of all defects increased with the increase in irradiation fluence. Among them, the growth rate of H_1 defect concentration was significantly higher than that of other defect types (H_2, H_3, H_4). When the radiation fluence reached 5×10^{15} cm^{-2}, the concentration of H_1 defects rose to 7.11×10^{14} cm^{-3}, while the concentrations of H_2, H_3, and H_4 defects respectively were 3.32×10^{13} cm^{-3}, 3.85×10^{13} cm^{-3}, and 2.84×10^{13} cm^{-3}. At this irradiation fluence, the concentration of H_1 defects was approximately 20 times that of other defect concentrations, indicating that the defects introduced by high-fluence 1-MeV electron irradiation were mainly H_1 defects. Moreover, by fitting with the Arrhenius formula (Fig. 9), the capture cross-section σ of H_1 defects reached 1.78×10^{-12} cm^2, which was much higher than that of other defect types. The substantial increase in H_1 concentration and its efficient recombination characteristics are thus a key factor in the rapid degradation of GaInP/GaAs HJT solar cells under high-fluence 1-MeV electron irradiation. As an efficient SRH recombination center, H_1 reduces carrier lifetime and diffusion length, diminishing the collection of photogenerated carriers. This leads to a significant increase in recombination current with irradiation fluence, consistent with the DIV analysis. Consequently, in the phot I–V test, the phenomenon of the electrical performance of GaInP/GaAs HJT cells rapidly degrading with the increase in irradiation fluence is manifested.

Based on the analysis of comprehensive literature data,[36,37] it was found that H_3 ($E_v+0.282$ eV) and H_4 ($E_v+0.032$ eV) in the GaInP/GaAs HJT cell might belong to the intrinsic point defect cluster. Their essence is that electron irradiation directly induces as lattice vacancies-interstitial atoms (V_{As}–I_{As}) through the displacement damage effect. Combined with the experimental results and theoretical analysis, H_1 ($E_v+0.717$ eV)/H_1^* ($E_v+0.744$ eV), and H_2 ($E_v+0.369$ eV) might originate from the migration of As interstitial atoms (I_{As}) induced by irradiation, and form defect complexes com-

bined with inherent impurities in the material.

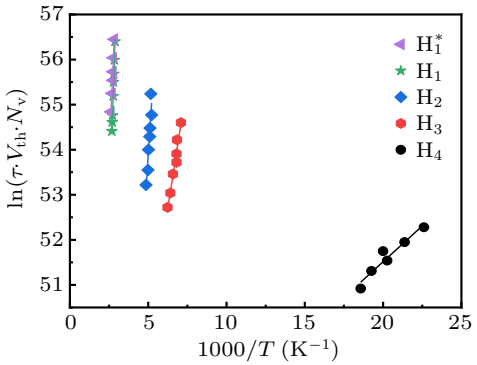


Fig. 9. Arrhenius fitting of various defects in GaInP/GaAs heterojunction solar cells after 1-MeV electron irradiation.

Table 3. 1-MeV electron radiation-induced defect energy levels and concentrations in GaInP/GaAs heterojunction solar cells by DLTS method.

		E_T–E_V (eV)	N_T (cm^{-3})	σ (cm^2)
5×10^{14} cm^{-2}	H_1	0.716	3.27×10^{13}	
	H_2	0.369	1.88×10^{13}	
	H_3	0.282	9.48×10^{12}	
	H_4	0.032	7.42×10^{12}	
1×10^{15} cm^{-2}	H_1^*	0.744	2.55×10^{14}	3.83×10^{-15}
	H_2	0.368	2.49×10^{13}	
	H_3	0.301	1.96×10^{13}	
	H_4	0.032	2.19×10^{13}	
5×10^{15} cm^{-2}	H_1	0.717	7.11×10^{14}	1.78×10^{-12}
	H_2	0.368	3.32×10^{13}	1.02×10^{-13}
	H_3	0.277	3.85×10^{13}	9.09×10^{-18}
	H_4	0.032	2.84×10^{13}	8.82×10^{-20}

4. Conclusion and perspectives

This study systematically investigated the radiation damage effect of GaInP/GaAs HJT solar cells under different irradiation fluences of 1-MeV electrons at room temperature. Through LIV and EQE tests, the degradation laws of the cell's electrical performance were analyzed. The results showed that the three key electrical performance parameters of the solar cell: open-circuit voltage (V_{oc}), short-circuit current density (J_{sc}), and maximum output power (P_{max}), followed the logarithm degradation law when subjected to the electron irradiation fluence. The rapid degradation of V_{oc} is an important factor causing the degradation of solar cell performance. Under the same radiation conditions, the degradation amplitude of J_{sc} is significantly smaller than that of V_{oc}, and the critical injection fluence of J_{sc} is 62 times that of V_{oc}. And the heterojunction cell shows better radiation resistance, mainly as its V_{oc} degradation rate with fluence increase is lower than the homojunction cell. The spectral response test results show that the radiation damage of 1-MeV electron to GaInP/GaAs HJT cells mainly manifests as long-waveband damage. The degradation amplitude increases with the accumulation of irradiation fluence, and the degradation process of photogenerated current density J_{ph} shows a trend of first slow and then fast. DIV reveals that after 1-MeV electron irradiation, the dark characteristic curve presents two typical features, and both the recombination current and diffusion current have an increasing relationship with the irradiation fluence. After analysis, it is found that the dark current of GaInP/GaAs HJT cells is dominated by the recombination current. DLTS test reveals that after 1-MeV electron irradiation, four characteristic hole defect peaks (H_1–H_4) are mainly introduced into the GaInP/GaAs cells. Their energy level positions are calculated as H_1 ($E_v+0.717$ eV)/H_1^* ($E_v+0.744$ eV), H_2 ($E_v+0.369$ eV), H_3 ($E_v+0.282$ eV), and H_4 ($E_v+0.032$ eV), and in the high fluence condition, the H_1 defect is an important factor causing the rapid degradation of the solar cell.

Acknowledgements

Project supported by Shanghai Aerospace Science and Technology Innovation Fund (Grant No. SAST2024-083), the National Natural Science Foundation of China (Grant Nos. U2341222, U2441248, 12275061, and 12075069), and the Fund for State Key Laboratory (Grant No. 6142806230204).

References

[1] Baur C, Khorenko V, Siefer G, Inguimbert V, Park S, Boizot B, Bourgoin J C, Casale M and Gras A 2017 *E3S Web of Conferences* 16 04005
[2] Khorenko V, Baur C, Siefer G, Schachtner M, Park S, Boizot B, Bourgoin J C, Casale M and Campesato 2017 *E3S Web of Conferences* **16** 03011
[3] Ulloa-Severino A, Carr G A, Clark D J, Orellana S M, Arellano R, Smart M C, Bugga R V, Boca A and Dawson S F 2017 *E3S Web of Conferences* **16** 13004
[4] Boca A, Warwick R, White B and Ewell R 2017 *IEEE J Photovolt.* **7** 1159
[5] Zhao Y, Zheng S Y, Zhao Y M, Luo Z J, Li Y M, Wu Y K, Chen J T, Chen J B, Zhang X Q, Chai L Q, Han X X, Xin H and Li Y 2023 *Appl. Phys. Lett.* **123** 233901
[6] Zhao Y, Bai Q Q, Chai L Q, Dong X F, Chen J, Chen J T, Li Y and Han X X 2022 *Adv. Mater. Interfaces* **9** 2201049
[7] Zhao Y, Bai Q Q, Liao P J, Ding X Q, Zuo X Y, Huang W F, Kuang G X, Zheng Y X, Chai L Q, Chen J T, Zhang X Q, Chen J B and Li Y 2023 *Phys. Lett. A* **472** 128804
[8] Bermudez-Garcia P, Voarino P and Raccurt O 2021 *Appl. Energy* **290** 116757
[9] Bolton S J, Lunine J, Stevenson D, Connerney J E P, Levin S, Owen T C, Bagenal F, Gautier D, Ingersoll A P, Orton G S, Guillot T, Hubbard W, Bloxham J, Coradini A, Stephens S K, Mokashi P, Thorne R and Thorpe R 2017 *Space Sci. Rev.* **213** 5
[10] Dawson S F, Stella P, McAlpine W and Smith B 2012 *Proceedings of the 10th International Energy Conversion Engineering Conference*, July 30–August 1, 2012 Atlanta, Georgia, USA, p. 3833
[11] Elfiky D, Yamaguchi M, Sasaki T, Takamoto T, Morioka C, Imaizumi M, Ohshima T, Sato S I, Elnawawy M, Eldesuky T and Ghtas A 2010 *Proceedings of the 35th IEEE Photovoltaic Specialists Conference*, June 20–25, 2010 Honolulu, HI, USA, p. 002528
[12] Green M A, Dunlop E D, Hohl-Ebinger J, Yoshita M, Kopidakis N and Hao X 2020 *Prog. Photovolt. Res. Appl.* **28** 629

[13] Wang Z J, Xue Y Y, Yang X, Cui X Y, Jia T X, Jiao Q L, Nie X and Lai S K 2021 *Nucl. Instrum. Methods Phys. Res. A* **1018** 165763

[14] Liu L, Mei B, Zheng Z S, Wang L, Bai Y R, Yu Q K, Li P, Zhao H D, Sun Y C and Li B 2023 *IEEE Trans. Nucl. Sci.* **70** 1885

[15] Raya-Armenta J M, Bazmohammadi N, Vasquez J C and Guerrero J M 2021 *Sol. Energy Mater. Sol. Cells* **233** 111379

[16] Takamoto T, Yamaguchi M, Taylor S J, Yang M J, Ikeda E and Kurita H 1999 *Sol. Energy Mater. Sol. Cells* **58** 265

[17] Yan G, Wang J L, Liu J, Liu Y Y, Wu R and Wang R 2020 *J. Lumin.* **219** 116905

[18] Wang T B, Wang Z X, Zhang S Y, Li M, Tang G H, Zhuang Y, Yang X and Aierken A 2024 *J. Appl. Phys.* **135** 053103

[19] Yang S S, Gao X, Feng Z Z, Zhang L and Cui X Y 2013 *Proc. RADECS* 2013 PI

[20] Liu H, Liu Q M, Liu J P, Zhao Y G, Yu Y J, An Y, Wei G H, Li Y Z, Fu Y J, Li J S and He D Y 2024 *Sol. Energy Mater. Sol. Cells* **264** 112624

[21] Cao M J, Wang Q, Shang J C, Zhou Y R, Dong G Q, Zhang L M, Li S H, Cui Y H, Liu F Z and Zhou Y Q 2024 *Sol. Energy Mater. Sol. Cells* **273** 112954

[22] Schulte K L, Simon J, Steiner M A and Ptak A J 2023 *Cell Rep. Phys. Sci.* **4** 101541

[23] Martí A 2019 *IEEE J. Photovolt.* **9** 1590

[24] Hwang S T, Kim S H, Cheun H S, Lee H, Lee B H, Hwang T H, Lee S H, Yoon W K, Lee H M and Park B W 2016 *Sol. Energy Mater. Sol. Cells* **155** 264

[25] Yang L, Hu Z C, He Q Y, Liu Z K, Zeng Y H, Yang L F, Yu X G and Yang D R 2024 *Sol. Energy Mater. Sol. Cells* **275** 113022

[26] Chen Q Y, Yang X R, Li Z Z, Bi J S, Xi K, Zhang Z X, Zhai P F, Sun Y M and Liu J 2023 *Chin. Phys. B* **32** 096102

[27] Feng Y H, Guo H X, Liu Y W, Ouyang X P, Zhang J X, Ma W Y, Zhang F Q, Bai R X, Ma X H and Hao Y 2024 *Chin. Phys. B* **33** 016104

[28] Zhong A X, Wang L, Tang Y, Yang Y T, Wang J J, Zhu H P, Wu Z P, Tang W H and Li B 2023 *Chin. Phys. B* **32** 076102

[29] Zhang Y Q, Wu Y Y, Zhao H J, Sun C Y, Xiao J D, Geng H B, Xue J W, Lu J F and Wang Y 2016 *Sol. Energy Mater. Sol. Cells* **157** 861

[30] Utamuradova Sh B, Terukov E I, Ataboev O K, Panaietti I E, Kabulov R R and Troshin A V 2025 *Nucl. Instrum. Methods Phys. Res. Sect. B* **560** 165630

[31] Zhou J M, Zhang Y Q, Liu C M, Li H Y, Qi C H, Wang T Q, Ma G L, Xiao L Y and Huo M X 2023 *Opt. Mater.* **146** 114540

[32] Imaizumi M, Nakamura T, Tajima M, Sato S I and Ohshima T 2013 *Proceedings of the 2013 IEEE 39th Photovoltaic Specialists Conference (PVSC)*, June 16–21, 2013 Tampa, FL, USA, p. 3243

[33] Tada H Y, Carter J R, Anspaugh B E and Downing R G 1982 *Solar Cell Radiation Handbook*, 3rd edn. (Pasadena: Jet Propulsion Laboratory) pp. 82–69

[34] Pellegrino C, Schön J, Lang R, Dimroth F, Zimmermann C G and Lackner D 2023 *Prog. Photovolt.* **31** 1051

[35] Wang Z X, Liu M Q, Wang T B, Zhang S Y, Li M, Tang G H, Zhuang Y, Yang X, Zhong L and Aierken A 2024 *Mater. Sci. Semicond. Process.* **171** 108033

[36] Pons D and Bourgoin J C 1985 *J. Phys. C Solid State Phys.* **18** 3839

[37] Stievenard D, Boddaert X and Bourgoin J C 1986 *Phys. Rev. B* **34** 4048